The pressure-induced phase transition of mechanically alloyed nanocrystalline GaSb

2008 J. Phys.: Condens. Matter 20 275212

(http://iopscience.iop.org/0953-8984/20/27/275212)

J. Phys.: Condens. Matter **20** (2008) 275212 (7pp) doi:10.1088/0953-8984/20/27/275212

The pressure-induced phase transition of mechanically alloyed nanocrystalline GaSb

C E M Campos[1], J C de Lima[1], T A Grandi[1], J P Itié[2], A Polian[3], J C Chervin[3], P S Pizani[4] and E B Saitovich[5]

[1] Departamento de Física, Universidade Federal de Santa Catarina, CP 476, 88 040-900 Florianópolis, SC, Brazil
[2] Synchrotron SOLEIL, L'Orme des Merisiers, St Aubin, BP 48, F-91192 Gif-Sur-Yvette, France
[3] Physique des Milieux Denses, IMPMC, CNRS, Unversité Pierre et Marie Curie Paris 6, 140 rue de Lourmel, 75015 Paris, France
[4] Departamento de Física, Universidade Federal de São Carlos, 13565-905 São Carlos, SP, Brazil
[5] Centro Brasileiro de Pesquisas Físicas, 22290-180 Rio de Janeiro, RJ, Brazil

E-mail: pcemc@fisica.ufsc.br

Received 6 February 2008, in final form 8 May 2008
Published 3 June 2008
Online at stacks.iop.org/JPhysCM/20/275212

Abstract

Ga K-edge energy dispersive x-ray absorption spectroscopy and Raman spectroscopy measurements were employed to follow the pressure-induced semiconductor–metal phase transition of nanocrystalline GaSb produced by mechanical alloying up to 26 GPa. The results showed a slight increase of the phase transition pressures for both as-milled (8 GPa) and annealed (10 GPa) GaSb samples, as compared to that for the bulk one. The extended x-ray absorption fine structure analysis of the zinc blende (ZB) pressure domain (<10 GPa) showed that the microscopic compressibility of the bonds in the as-milled/annealed samples is higher/lower than the crystalline bulk modulus (56 GPa). The comparison between x-ray absorption near edge structure regions of the spectra and multiple scattering calculations suggests that the ZB structure evolves to a short-range chemically ordered β-Sn structure for pressures as high as 8 GPa. Raman measurements confirm the semiconductor–metal phase transitions of ZB-GaSb between 8 and 11 GPa for both as-milled and annealed samples, showing that the semiconductor character was not recovered on releasing the pressure down to 3.9 and 1.8 GPa, indicating a very strong hysteresis effect (or even irreversible transitions). The well-known transverse effective charge reduction with pressure was also observed. Furthermore, resonance behaviour is clearly seen for transverse optical phonons and the resonance maxima peak occurs at about 1.2 GPa, corresponding to 2.11 eV in the E_1 scale, smaller by 0.3 eV than the incident photon energy.

1. Introduction

Gallium antimonide (GaSb), the less ionic of the III–V semiconductors, has been extensively studied under high pressure conditions due to its similarity with the group IV elements (Si and Ge) and because different phase transition schemes (phases and pressures) were reported in the literature. Moreover, it is the only one among the III–V and II–VI binary semiconductors to have a lack of long-range order in all of the high pressure phases reported to date [1]. GaSb is also a potential candidate to test several theoretical models, involving *ab initio* and phenomenological considerations, designed to predict its local structure and vibrational states investigated by x-ray absorption spectroscopy (XAS) and Raman experiments [2–4].

In the III–V systems, such as GaX and InX (X = P, As, Sb), two phase transition schemes have been proposed (i) for the less ionic GaX and InSb compounds: zinc blende (ZB) →

β-Sn $\rightarrow$ hexagonal, and (ii) for the more ionic InAs and InP compounds: ZB $\rightarrow$ NaCl $\rightarrow$ β-Sn [5, 6]. However, angle dispersive x-ray diffraction (ADXRD) has led to a serious reevaluation of these transition schemes [7, 8].

In an energy dispersive x-ray diffraction study [9] several phase transitions of GaSb were reported up to 110 GPa, the highest pressure to which III–V compounds have been studied. The first transformation from the zinc blende to the β-Sn structure was confirmed and followed by a transformation to a simple hexagonal (SH) structure at 28 GPa on loading and 25 GPa on unloading. This was the first example of a SH structure in an III–V compound and it occurs at lower pressure than predicted by *ab initio* pseudopotential total-energy calculations (52.8 GPa) [3]. Upon a further increase in pressure, the authors reported that the simple hexagonal structure transformed to another structure (supposed disordered orthorhombic one) at 61 GPa which persisted up to 110 GPa. A large hysteresis associated with this last transition was reported [9]. In another paper [10] the zinc blende phase transition to a diatomic equivalent of β-Sn (fractional coordinate $u = 0.25$) has been proposed based on the similarities with the phase diagram of other III–V compounds and experimental EXAFS data.

In [11] the well-documented transition at 7 GPa was suggested to be to a disordered orthorhombic structure with space group $Imma$, rather than to the β-Sn structure previously reported [8]. The stability range proposed for the $Imma$ phase was of the order of 50 GPa [12], some 20 times that of the $Imma$ phase in Si. Mezouar *et al* [13] have found a site-disordered β-Sn phase, and concluded that the occurrence of the $Imma$ phase was due to non-hydrostatic conditions in the pressure cell. A recent paper [14] has shown that heating the $Imma$ phase at pressures up to $\sim$13 GPa results in a transformation to the β-Sn structure, which suggests that β-Sn is indeed the stable phase in this pressure range. When the $Imma$ phase is heated at pressures above $\sim$13 GPa a new $Ammm$ phase appears, mixed with β-Sn phase below $\sim$20 GPa, remaining stable at room temperature. This is also a disordered orthorhombic structure (quasi-monoatomic), closely related to the $Imma$ structure.

The more recent pressure phase diagrams for III–V semiconductors recognize the occurrence of the low symmetry orthorhombic structures with space groups $Cmcm$ or $Imm2$ and $Imma$. Furthermore, the most recent ADXRD results evidenced a long-range site-disorder at high pressure; which do not exclude the possibility of ordering over a short-range scale, as observed for GaP by XANES calculations/analysis [8].

The goal of the present paper is to follow the semiconductor–metal phase transition of nanocrystalline GaSb produced by mechanical alloying (MA) [15] (MA-GaSb) using energy dispersive x-ray absorption spectroscopy (XAS) and Raman spectroscopy and to compare some physical properties with those measured after annealing, as well as with those of standard bulk and nanostructures produced by different techniques. An insight on the short-range chemical ordering based on *ab initio* calculations of the XANES profiles is also presented.

2. Experimental procedure

The cubic zinc blende GaSb phase was produced by mechanical alloying technique [15] (it will be called MA-GaSb), which is a solid state route based on the action of non-hydrostatic pressures. The x-ray diffraction pattern of the MA-GaSb sample showed a GaSb phase that was indexed as a ZB structure with space group $F\bar{4}3m$ and a lattice parameter 6.086 Å (refined by the Rietveld method). A small portion of the MA sample was submitted to thermal annealing at 600 °C for 2 h and 30 min (it will be called ta-MA-GaSb). The annealing effect was only promoting structural relaxation, removing point and line defects, as well as stress and strain, growth of grain size and segregation of the Sb particles. The mean crystallite size and strain for the GaSb phase, calculated using the Williamson–Hall approach, were $\sim$13 nm and 3.0% for MA-GaSb and $\sim$26 nm and 0.9% for ta-MA-GaSb. More details about samples preparation and their structural, thermal and optical characterizations can be found in our previous studies [15]. Chemical analyses of the samples were performed by x-ray fluorescence (EDX), showing a slight deviation from the equiatomic composition (54 at.% Ga).

Chervin-type and B-05 DiaCell diamond anvil cells (DACs) were used as pressure generators for Raman and XAS experiments, respectively. The gasket was stainless steel and the size of the hole was approximately 200 μm. Neon gas and methanol/ethanol/water mixture (16:3:1) were used as pressure transmitting medium in Raman and XAS experiments, respectively. Although we carried out two distinct experiments with two distinct DACs, the loading conditions were kept the most similar as possible. The pressure determination during both experiments was performed through the pressure-dependent fluorescence of a ruby chip.

XAS measurements were performed at the Brazilian synchrotron radiation laboratory (LNLS) on D06A beamline at the gallium K edge ($E = 10\,367$ eV). The beam was focussed by a curved polychromator Si(111) crystal in Bragg geometry and vertically with a bent Si mirror placed at 2.8 mrad respect to the direct beam. The size of the spot at the sample position was $\sim$150 μm horizontally and vertically. The Bragg diffraction peaks arising from the diamond anvils were removed from the energy range of interest by changing the orientation of the diamond anvil cell and following in real time the intensity of the transmitted beam on a two-dimensional CCD detector. In this case the k range was limited to $\sim$10 Å^{-1}. The data were recorded at room temperature. The maximum pressure reached was 13 GPa.

The EXAFS data analysis was performed using the codes from the iFEFFit package [16]. The experimental EXAFS functions were obtained after subtracting the embedded-atom absorption background from the measured absorption coefficient and normalizing by the edge step using the program ATHENA [17]. Phase shifts for photoabsorber and backscatterer atoms have been calculated using FEFF6 [18]. Structural data for the GaSb phases used by the ATOMS program [19] to prepare the input for FEFF6 and FEFF8 [20] (XANES) were taken from ICSD [21], references [8, 10] for β-Sn structure and [14] for $Imma$ structure.

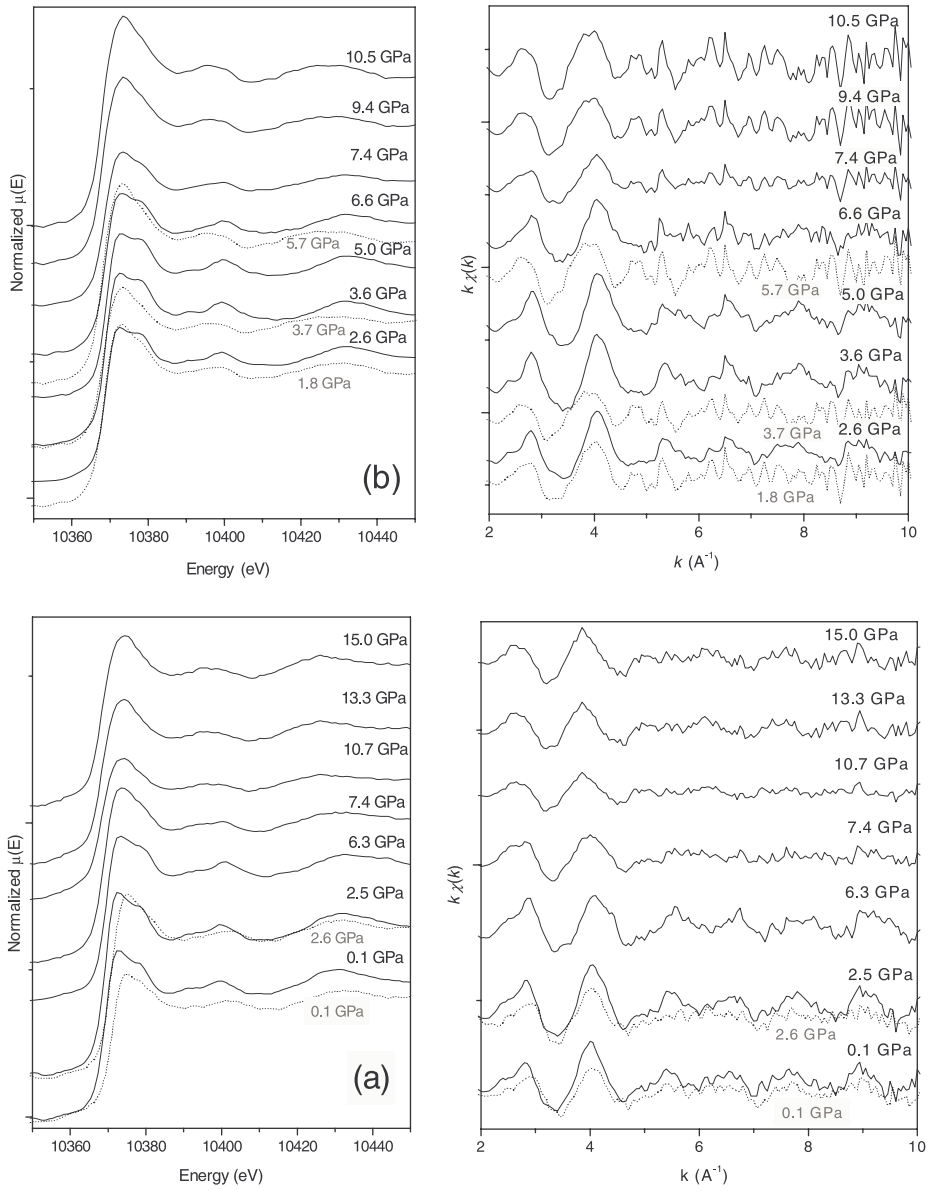

Figure 1. XANES (left panels) and EXAFS (right panels) spectra of MA-GaSb (a) and ta-MA-GaSb (b) samples as a function of pressure. Dotted lines represent the spectra collected during pressure release.

The diamond Bragg peaks limited the available spectral range for the high pressure gallium K-edge EXAFS spectra to a wavevector, k, of 10 Å^{-1} whereas for room-pressure data (no DACs) k_{max} can be larger than 20 Å^{-1}. The narrowing of the available spectral range decreases the number of independent structural parameters, which may be obtained by EXAFS. For this reason we fixed the coordination numbers for fitting the high pressure data.

Raman scattering measurements were performed at ambient temperature using a XY Dilor triple monochromator, in the subtractive mode, coupled to optical focal lens (20×) and CCD detecting system. This set up give a band-pass of 2 cm^{-1} at the Raman peak position. The 514.5 nm line of an argon ion laser was used as exciting light in backscattering geometry and using an output power below 5 mW to avoid overheating of sample.

3. Results and discussions

3.1. XAS measurements

Figure 1 (left panels) shows the XANES region of the normalized XAS spectra of MA-GaSb (a) and ta-MA-GaSb (b) samples as a function of pressure, while the right panels show the k-weighted EXAFS oscillations for both samples in k space at same pressures. From this figure one can observe a typical four-fold coordination XANES profile for 'low' pressures (up to 6.6 GPa (b) and 6.3 GPa (a)) spectra of both samples. Above this pressure (at 7.4 GPa for both samples), the shape of the XANES begins to change, loosing the second maximum occurring just above the absorption edge, and the first oscillation after the edge broadens. Such modifications of the XANES are characteristic of the onset of a transition from a four-fold to a six-fold coordination scheme. The transition

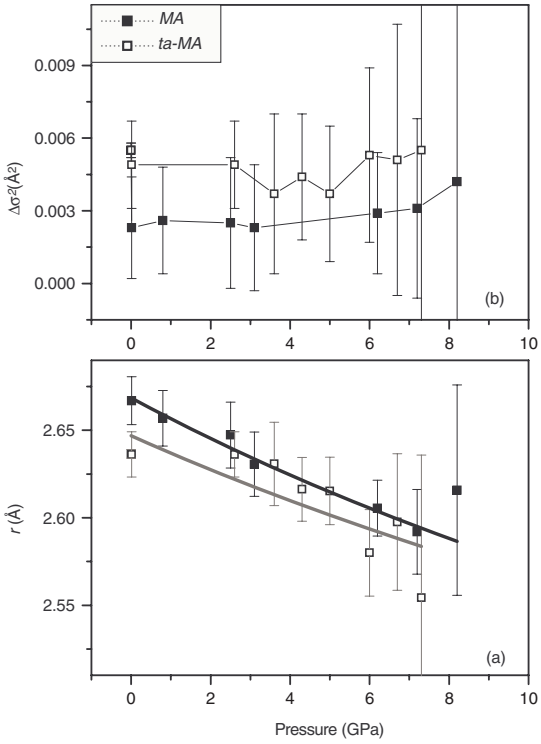

Figure 2. The nearest-neighbour interatomic distances r (a) and pseudo-Debye–Waller factors (b) of the MA-GaSb and ta-MA-GaSb samples as a function of pressure. Thick lines show the fittings with Murnaghan's equation.

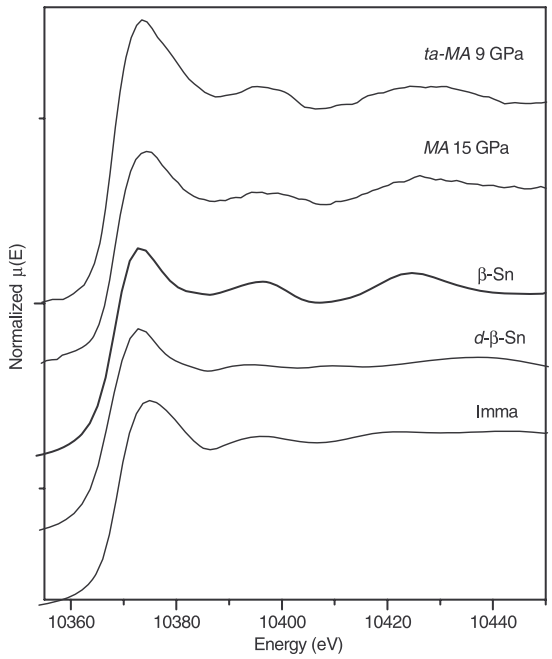

Figure 3. Experimental XANES data of the MA-GaSb and ta-MA-GaSb samples at 15 GPa and 9 GPa, respectively compared with calculated spectra of GaSb in the β-Sn, disordered-β-Sn and *Imma* structures.

range is clearly seen by the lost of the oscillations, which are observed below 6.6 GPa and again above 9 GPa.

Figure 2 shows the nearest-neighbour interatomic distances r (a) and pseudo-Debye–Waller factors (b) of the MA-GaSb and ta-MA-GaSb samples as a function of pressure. The bond length dispersion increases as a function of pressure, i.e., as the phase transition takes place and signal-to-noise ratio decreases (figure 2(b)). The EXAFS analysis in the ZB (zinc blende) pressure domain (<10 GPa) showed a pseudo-Debye–Waller factor (local disorder) almost constant to the experimental accuracy and interatomic distance decreasing with pressure. The highest pressure point shown here for MA-GaSb presents an increase both in interatomic distance and in the pseudo-Debye factor. These two observations are consistent with the onset of the phase transformation. The microscopic compressibility of the bonds and its derivate (B_o and B', respectively) were extracted from the fitting of the Murnaghan's equation (equation (1)) to the distance data d versus pressure P.

$$d(P) = d_o\left(1 + \frac{B'P}{B_o}\right)^{\frac{-1}{3B'}}. \qquad (1)$$

The results obtained were $B_o = 72 \pm 3$ ($B' = 4$) for the MA-GaSb sample and $B_o = 87 \pm 26$ ($B' = 4$) for the ta-MA-GaSb sample. The microscopic compressibility for both samples is higher than the crystalline bulk modulus reported in the literature: $B_o = 56.7$–58 GPa [22, 23]. The literature also reported a huge difference between the microscopic and macroscopic bulk modulus of an amorphous GaSb (105 ± 20 GPa and 35 GPa, respectively) that was attributed as an unambiguous evidence for a pressure-induced geometrical or topological distortion in the amorphous GaSb tetrahedral network [24]. Then, the as-milled and annealed samples here in have similarities with microscopic bulk modulus of an amorphous specimen, probably due to their highly disordered interfacial component.

3.2. XANES calculations

A self-consistent energy-dependent exchange correlation Hedin–Lundqvist potential was used in the FEFF 8 code [20] to simulate the XANES spectra of high pressure MA-GaSb and ta-MA-GaSb samples. The radius of (atoms sum in) cluster for full multiple scattering during the self-consistency loop were 5.5 Å (27) for ordered/disordered β-Sn and 5.7 Å (43) for ordered *Imma* structures, respectively. Full multiple scattering XANES calculations up to a photoelectron wavevector value of $k = 6$ Å^{-1} (corresponding to an energy of about ∼130 eV) were carried out for a larger cluster of atoms centred on the photoabsorber of a radius of 6.2 Å (57 atoms) for β-Sn and 7 Å (73 atoms) for *Imma* structures. All multiple scattering paths with these clusters were summed to infinite order. No thermal or static disorder factor was added to the simulations, the only external parameters used as input for the simulations were a constant experimental broadening and an offset in the energy scale.

Figure 3 shows the experimental XANES data of the MA-GaSb at 15 GPa, ta-MA-GaSb at 9 GPa and the calculated spectra of GaSb in the chemically ordered β-Sn, chemically disordered β-Sn and *Imma* structures. From this figure, it can

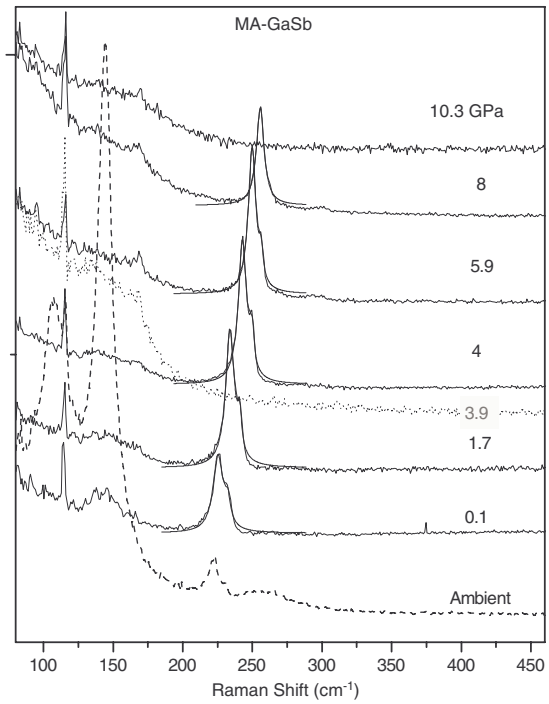

Figure 4. Raman spectra of the MA-GaSb sample as a function of pressure. The dotted line represents the spectrum collected during pressure release. The line on the LO–TO band represents the fit to determine the frequencies.

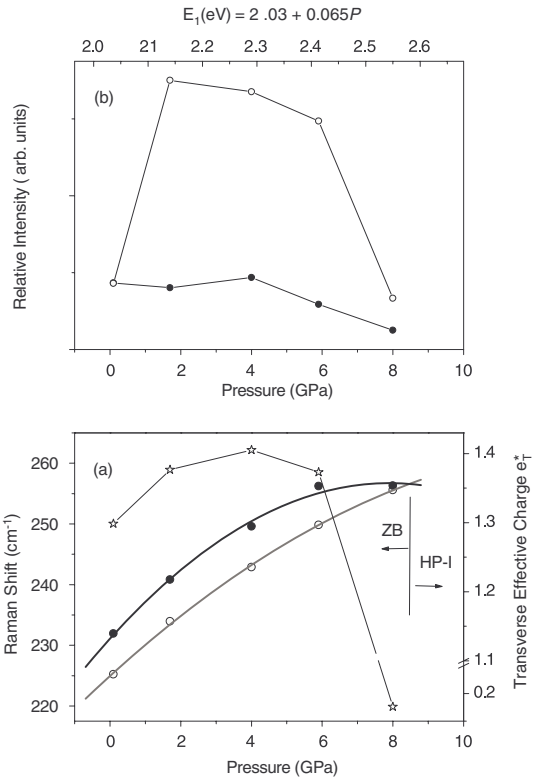

Figure 5. (a) Dependence of the TO- (empty circles) and LO-phonon frequencies (full circles) of the MA-GaSb on pressure. Solid lines are polynomial fits to the experimental data. Representative error bars are shown for two Raman lines. The right side scale shows the transverse effective charge e_T^* (stars) as a function of pressure. (b) Dependence of the TO- (empty circles) and LO-phonon scattering on pressure (lower scale) and E_1 gap (upper scale) [25].

be seen that the rounded-like shape of the post-edge XANES features are obtained for all structures mentioned above, but a better matching between other features (peaks and valleys) suggests that the chemically ordered β-Sn is the most probable high pressure phase for both samples. It is important to remember that several reports, such as [13], have evidenced the importance of the pressure medium and of micro-strains on this kind of phase transition, which can modifies the structure at high pressure.

3.3. Raman measurements

Figure 4 shows the Raman spectra of MA-GaSb sample as a function of pressure. From this figure one can identify in the 200–250 cm^{-1} range the longitudinal and transversal optical phonons (LO and TO, respectively) of ZB-GaSb phase. Moreover, very intense low frequency features (<170 cm^{-1}) can be seen in the spectrum at ambient conditions (inside the DAC). These features stand in the spectral region of A_{1g} and E_g optical modes of rhombohedral Sb. However, critical comments have already been done [15] contesting the attribution of the low frequency features just to Sb optical phonons, where metastable phase(s) were proposed.

The identification of both LO and TO GaSb modes was perturbed with pressure increase because they almost collapsed into a single broad line, showing different pressure dependence and consequently decreasing of the transversal effective charge e_T^* of Ga–Sb bonds (ionic character, calculated from equation (2) [25]) with pressure (see right y-axis in figure 5(a)). The very intense Raman features of non-reacted Sb and/or metastable phase(s) found at ambient conditions practically vanished under high pressure. For pressures larger than 8 GPa no more Raman active modes could be detected, confirming a semiconductor–metallic phase transition. The semiconductor character of the MA-GaSb sample was not recovered during pressure release (down to 3.9 GPa), indicating very strong hysteresis effect or even an irreversible transition. Figure 5(a) shows the pressure dependence of the frequency of the most intense Raman lines of the MA-GaSb sample. Fittings were done for the peak positions of TO and LO modes using second order polynomial functions.

The results of the fit are (frequencies in cm^{-1} and pressures in GPa):

$$\omega_{TO} = 224.9 + 5.3P - 0.19P^2$$
$$\omega_{LO} = 231.1 + 6.5P - 0.41P^2.$$

The transverse dynamic charge was calculated from the following equation

$$e_T^{*2} = \frac{\Omega M}{\varepsilon_\infty(\omega_{LO}^2 - \omega_{TO}^2)}, \qquad (2)$$

where Ω is the volume of the unit cell, M is the reduced mass, ε_∞ is the infrared dielectric constant and $\omega_{LO(TO)}$ are the LO-

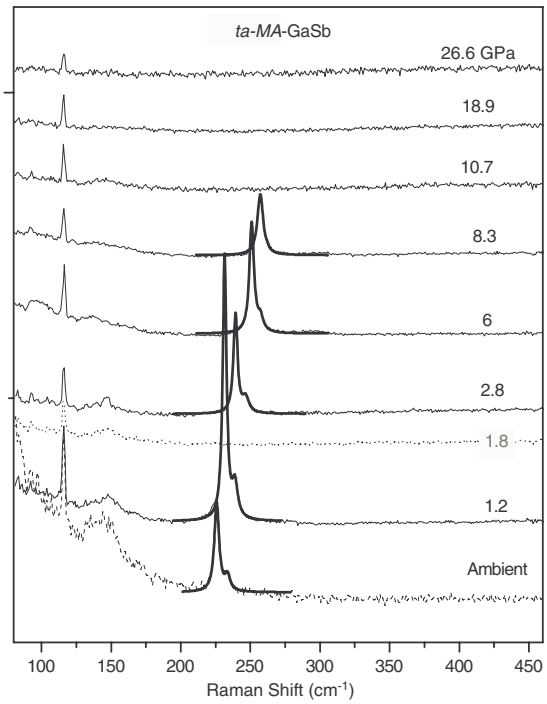

Figure 6. Raman spectra of the thermal annealed sample (ta-MA-GaSb) as a function of pressure. The dotted line represents the spectrum collected during pressure release.

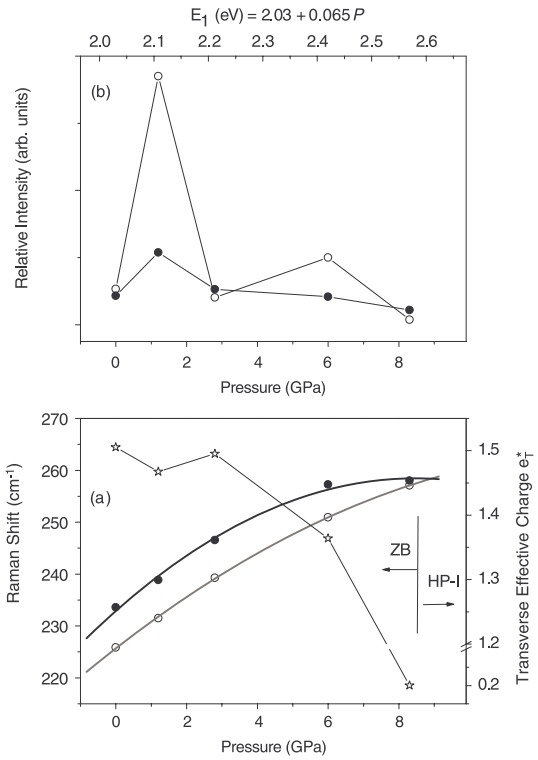

Figure 7. The same as figure 5 but for the ta-MA-GaSb sample.

(TO-)phonon frequencies. No changes of the primitive-unit-cell volume with pressure were considered.

Figure 5(b) shows the variation of the Raman scattering intensity (i.e. peak height ignoring any change in linewidth with pressure) in MA-GaSb with pressure (lower scale) and the corresponding E_1 gap energy (upper scale) extracted from [25]. The resonance behaviour is clearly seen in TO phonons (empty circles). As the E_1 gap approaches the incident photon energy with increasing pressure, the scattering intensity is enhanced due resonance effects. The resonance maximum occurs at 1.7 GPa, at which pressure the gap is $E_1 = 2.14$ eV, smaller by 0.25 eV than the incident photon energy of 2.41 eV (514.5 nm). This comparison is merely indicative since the values used in calculations of E_1 were not obtained from our sample.

Figure 6 shows the Raman spectra of the ta-MA-GaSb sample as a function of the pressure. At ambient conditions almost the same features as those for the as-milled sample are observed. The most notable differences observed after annealing are the enormous intensity increasing of both optical modes and the recovering of the bulk-like parameters. The semiconductor–metallic phase transition in the ta-MA-GaSb sample occurs between 8.3 and 10.7 GPa as indicated from the disappearing of the Raman modes. It is interesting to note that no reversibility of this phase transition was observed immediately after releasing the pressure to 1.8 GPa.

Figure 7(a) shows the pressure dependence of the optical modes and the transverse effective charge (right y-axis) of the ta-MA-GaSb sample. The TO and LO modes pressure dependences of the ta-MA-GaSb were fitted by second order polynomials as:

$$\omega_{\mathrm{TO}} = 225.7 + 5.3P - 0.18P^2$$

$$\omega_{\mathrm{LO}} = 232.9 + 6.0P - 0.36P^2.$$

The found coefficients are smaller than those of MA-GaSb and larger than those (4.67(13) and $-0.11(2)$ cm^{-1} GPa^{-2} for TO and 4.56(13) and $-0.12(2)$ cm^{-1} GPa^{-2} for LO) reported for a GaSb bulk sample [25].

Figure 7(b) shows the variation of the Raman scattering intensity in ta-MA-GaSb with pressure (lower scale) and the corresponding E_1 gap energy (upper scale). The resonance behaviour is clearly seen in TO phonons. As the value of the E_1 gap is pressure tuned in the vicinity of the incident photon energy with increasing pressure, the scattering intensity is enhanced due resonance effects. The resonance maxima peak occurs at 1.2 GPa, corresponding to 2.11 eV in E_1 scale, smaller by 0.30 eV than the incident photon energy.

4. Conclusions

The short-range structural and vibrational studies of the MA-GaSb and ta-MA-GaSb samples as submitted to high pressure conditions were done and the main conclusions are:

- The phase transition of the MA-GaSb was observed for pressures higher than those of bulk samples, remaining almost 1–2 GPa higher even after annealing at 600 °C for 150 min (ta-MA-GaSb sample). A fit of the first neighbours distance with a Murnaghan's equation gives

linear compressibilities B_o of 72 ± 3 and 87 ± 26 GPa for ZB phases in the MA-GaSb and ta-MA-GaSb samples, respectively, which are between the bulk modulus for amorphous (microscopic one) and crystalline GaSb.

- XANES calculations suggests that the first high pressure phase is a site ordered β-Sn.
- Semiconductor–metal phase transitions of ZB-GaSb were observed between 8 and 11 GPa for both MA-GaSb and ta-MA-GaSb samples, which semiconductor character were not recovered on pressure release down to 3.9 and 1.8 GPa, indicating very strong hysteresis effect. The LO mode of MA-GaSb is less dispersive than that of bulk one, but after annealing the mechanically alloyed sample showed values comparable to those of bulk samples. Moreover, transverse effective charges for both samples showed strong reduction as pressure increase. As the E_1 gap approaches the incident photon energy with increasing pressure, the scattering intensity, mainly of TO modes, were enhanced due resonance effects.

Acknowledgments

We wish to thank Brazilian and French agencies (CNPq, CAPES and COFECUB) for financial support. We are also indebt with B Canny (IPMC/Paris VI) for their helpful technical support in the Raman measurements under pressure. The XAS experiments were performed thanks to LNLS facilities in the DXAS 4786/05 and XAFS 5728/06 projects.

References

[1] Vanpeteghem C B, Nelmes R J, Allan D R, McMahon M I, Sapelkin A V and Bayliss S C 2001 *Phys. Status Solidi* b **223** 405
[2] Libotte H and Gaspard J P 2003 *Europhys. Lett.* **63** 545
[3] Zhang S B and Cohen M L 1987 *Phys. Rev.* B **35** 7604
[4] Trallero-Giner C, Kunc K and Syassen K 2006 *Phys. Rev.* B **73** 205202
[5] Ozoliņš V and Zunger A 1999 *Phys. Rev. Lett.* **82** 767
[6] Mujica A, Rubio A, Muñoz A and Needs R J 2003 *Rev. Mod. Phys.* **75** 863
[7] Nelmes R J and McMahon M I 1994 *J. Synchrotron Radiat.* **1** 69
[8] Aquilanti G, Libotte H, Crichton W A, Pascarelli S, Trapananti A and Itié J P 2007 *Phys. Rev.* B **76** 064103
[9] Weir S T, Vohra Y K and Ruoff A L 1987 *Phys. Rev.* B **36** 4543
[10] San-Miguel A, Itié J P and Polian A 1995 *Physica* B **208** 506
[11] McMahon M I, Nelmes R J, Wright N G and Allan D R 1994 *Phys. Rev.* B **50** 13047
[12] Nelmes R J, McMahon M I, Wright N G, Allan D R, Liu H and Loveday J S 1994 *J. Phys. Chem. Solids* **56** 539
[13] Mezouar M, Libotte H, Députier S, Le Bihan T and Häusermann D 1999 *Phys. Status Solidi* b **211** 395
[14] Vanpeteghem C B, Nelmes R J, Allan D R and McMahon M I 2002 *Phys. Rev.* B **65** 012105
[15] Campos C E M, de Lima J C, Grandi T A, Schimitt M and Pizani P S 2006 *J. Phys.: Condens. Matter* **18** 8613
[16] Newville M 2001 *J. Synchrotron Radiat.* **8** 322
[17] Ravel B and Newville M 2005 *J. Synchrotron Radiat.* **12** 537
[18] Zabinsky S I, Rehr J J, Ankudinov A, Albers R C and Eller M J 1995 *Phys. Rev.* B **52** 2995
[19] Ravel B 2001 *J. Synchrotron Radiat.* **8** 314
[20] Ankudinov A L, Ravel B, Rehr J J and Conradson S D 1998 *Phys. Rev.* B **58** 7565
[21] Inorganic Crystal Structure Database 2007 *(ICSD)* Gmelin-Institut für Anorganische Chemie and Fachinformationszentrum FIZ Karlsruhe
[22] Al-Douri Y *Pdf file in the web* yaldouri@yahoo.com
[23] Cohen M L 1985 *Phys. Rev.* B **32** 7988
[24] Lyapin A G, Brazhkin V V, Bayliss S C, Sapelkin A V, Itié J P, Polian A and Clark S M 1996 *Phys. Rev.* B **54** 14242
[25] Aoki K, Anastassakis E and Cardona M 1984 *Phys. Rev.* B **30** 681